View metadata, citation and similar papers at core.ac.uk
brought to you by CORE
provided by Infoscience - École polytechnique fédérale de Lausanne

MAGNETIC RESONANCE IN MEDICINE

Broadband Decoupled, ^{1}H-Localized ^{13}C MRS of the Human Brain at 4 Tesla

Rolf Gruetter, Gregor Adriany, Hellmut Merkle, Peter M. Andersen

Broadband proton decoupling of the entire ^{13}C spectrum was possible within power absorption guidelines and resulted in the detection of narrow (as low as 2–3 Hz), natural abundance signals from metabolites such as *myo*-inositol, glutamate, *N*-acetyl-aspartate, and glutamine from 72 cm^3 volumes in the human brain. To overcome the chemical shift displacement error, three-dimensional localization on the ^{1}H *z* magnetization was combined with polarization transfer. Efficiency of the heteronuclear localization method was demonstrated by the elimination of all scalp lipid resonances. A signal-to-noise ratio of 5:1 for 0.07 m*M* [^{13}C] was achieved in 12 min, which is approximately a fivefold improvement over the sensitivity reported at 2.1 Tesla.

Key words: ^{13}C MRS; human brain; polarization transfer; decoupling.

INTRODUCTION

A number of metabolites can potentially be measured by ^{1}H MRS, (1). However, the ^{1}H NMR spectrum is complicated by the presence of homonuclear coupling, which can spread peak intensities over a significantly large frequency range. This increased potential for spectral overlap is accentuated by the fact that the chemical shift range for carbon-bound aliphatic protons is typically only 5 ppm *in vivo*.

Despite its low sensitivity, broadband decoupled, ^{13}C MRS has a number of distinct advantages over ^{1}H MRS in that the resulting spectrum is generally much better resolved, contains mostly singlet peaks and thus simplified spectral appearances. These advantages, plus a well defined baseline and the absence of an intense water peak improve the chances of an accurate quantification of peak intensities. ^{13}C MRS was first used in the quantification of glucose (2) as well as *myo*-inositol (3) in the human brain. In addition, the novel observation of homonuclear couplings in glutamate *in vivo* after infusion of ^{13}C labeled substrates due to exchange reactions with tri-carboxylic acid cycle intermediates may yield important information on cerebral metabolic pathways (4, 5).

Only a few systematic broadband decoupled ^{13}C MRS studies of human brain *in vivo* have been reported (2, 3, 5). Most of the proton decoupled ^{13}C MRS research in humans has been focused on measuring liver glycogen, present in the several 100 m*M* concentration range, with regular publications from a few groups, e.g., refs. 6–8. Additional, more methodologically oriented papers from several groups have appeared (9–15), which indicates the increased technical obstacles that need to be solved for successful proton decoupled ^{13}C MRS.

Most of the brain studies using ^{13}C MRS have been performed on either animals, extracts, or brain slices, which has yielded important and valuable information on cerebral metabolism and compartmentation, see, e.g., ref. 16 and references therein. In addition to the wealth of information provided by these studies, it is highly desirable to extend these measurements to humans, since the compartmentalization of metabolism may be intricately linked to basic brain function, i.e., neurotransmission.

The apparent lack of ^{13}C NMR studies of the human brain can be explained partly by the difficulties that need to be overcome to apply ^{13}C MRS to humans. Most importantly, the requirement to broadband decouple the ^{13}C NMR spectrum within power absorption guidelines can impose a severe restriction on experimental design that is not present in extract analysis and animal experimentation. In addition, the *in vivo* application requires spatial localization, which is hard to achieve in ^{13}C NMR, because the large chemical shift dispersion and associated chemical shift displacement error might confine accurate localization to a range of 20 ppm when using homonuclear localization methods.

These problems are assumed to increase with higher field strengths, since the bandwidth needed for decoupling is proportional to B_o, as is the chemical shift displacement error. The present paper shows that these problems can be overcome at 4 Tesla in humans by using ^{1}H NMR localization combined with polarization transfer and broadband proton decoupling. The resulting sensitivity enabled observation of natural abundance peaks above the noise floor from metabolites such as glutamine in 12 min, which has an *in vivo* concentration of approximately 4 m*M*. The implied potential to study focal human brain function using ^{13}C MRS is discussed.

MATERIALS AND METHODS

All experiments were conducted on a 4 Tesla magnet with a 125-cm bore and a standard Siemens Magnetom Vision gradient coil (Siemens, Erlangen, Germany), presently capable of switching 23 mT/m in 1.2 μs, interfaced to a Varian/SISCO console (Varian, Palo Alto, CA). Four healthy human subjects were studied after giving informed consent according to procedures approved by the IRB:local human subjects committee.

The subjects were placed supine onto the patient bed with the carbon coil covering the occipital region. Posi-

MRM 36:659–664 (1996)

From the Clinical Research Center and Center for MR Research, Department of Radiology, University of Minnesota, Minneapolis, Minnesota.

Address correspondence to: Rolf Gruetter, Ph.D., Clinical Research Center and Center for MR Research, Department of Radiology, 385 E. River Road, Minneapolis, MN 55455.

Received April 15, 1996; revised July 30, 1996; accepted July 31, 1996.

This work was supported in part by U.S. Public Health Services grant RR07089, Biotechnological Research Resources Program, and by a grant from the Minnesota Medical Foundation MRF 107–95.

0740-3194/96 $3.00

Copyright © 1996 by Williams & Wilkins
All rights of reproduction in any form reserved.

tioning and localization were defined based on either T_1-weighted modified driven equilibrium Fourier transform (MDEFT) imaging with an inversion time TI = 1.2 s, echo time TE = 5.5 μs (17) or on fast low-angle shot (FLASH) imaging (TR = 60 μs, TE = 7 μs, α = 90°), (18). The position of a 72-ml volume (6 × 2 × 6 cm) in the occipital lobe was determined based on these multislice images and a larger region of at least 5 × 3 × 5 cm was shimmed by using a modification of the fast, automatic shimming technique by mapping along projections, FASTMAP (19), which allowed for anisotropic sampling of the volume of interest, resulting in 7–9 Hz water linewidth.

The system was equipped with two RF channels. The inputs of the decouple and the observe RF amplifiers were filtered with a ^{1}H bandpass filter and a low-pass filter, respectively. The amplifier outputs were fed into the magnet room through a filter plate and a ^{1}H band pass filter was inserted at the magnet into the decoupler path. A low-pass filter with 75 MHz cut-off frequency was inserted between the ^{13}C coil port and the transmit/receive switch. The filters were purchased from FSY Electronics Inc, Rockville, MD. Insertion loss of the filter was assessed by using a HP4396A network analyzer (Hewlett-Packard, Palo Alto, CA) to be 0.1 dB in the ^{13}C channel. This configuration alone provided at least 60 dB rejection of the mutual frequencies.

Proton decoupler power was calibrated at the input transmit port of the quadrature hybrid by using a high-power attenuator by measuring peak-to-peak voltage of the oscilloscope readings during long decoupler pulse trains and by measuring the peak power with a meter (Rohde & Schwarz, München, Germany).

The RF coil assembly consisted of a quadrature outer proton coil, driven with a quadrature hybrid (20). The coil was mounted on a curved acrylic glass cylinder. The inner ^{13}C surface coil consisted of a single loop with 7 cm diameter, and a balanced-match output circuit. Mutual electrical isolation at the two frequencies and respective coil ports was assessed to be at least 20 dB across the coil. The two 12-cm diameter ^{1}H coils maintained a distance of at least 1.5 cm to the tissue, which reduced high flux regions in the head to a minimum as verified by multislice ^{1}H imaging. In addition to the imaging, the B_1 field distribution was mapped by measuring the envelope of a series of one-dimensional projections along different projections, using the FASTMAP method (19). Incrementing the power produced B_1 plots that indicated that the maximum ^{1}H RF field was at the ^{13}C coil center (20).

RF power for the ^{13}C transmitter was kept at 580 W, and we adjusted the pulse width of a hard pulse to minimize the signal of a sphere containing ^{13}C labeled formic acid placed at the ^{13}C coil center. The pulse width varied at most by 20% with a mean of 90 μs for a signal null, equivalent to a $\gamma B_1/2\pi$ of approximately 5 kHz at coil center. This adjustment provided an assessment of the reproducibility of coil loading.

The decoupler power was adjusted on the formate signal by using the sequence 90° (^{13}C)-1/2J-θ(^{1}H)-acquire, as described previously (3), by minimizing the formate signal using a 500-μs 90° pulse (θ) on the formic acid peak. An additional power adjustment was performed for a 250-μs 90° (^{1}H) pulse. The power setting of the latter provided the basis for calculating the pulse widths for the ^{1}H pulses of the polarization transfer sequence and the inversion pulses, whereas the power setting for the former pulse was typically 30 Watts, which was set equal to the power used for broadband ^{1}H decoupling.

As in previous studies (2, 3, 5), ^{1}H decoupling was performed by using WALTZ-16 at the power level determined by the 500-μs 90° pulse at the ^{13}C coil center. The WALTZ-16 scheme was used with a 670-μs 90° pulse element, which was verified to provide complete decoupling of the entire ^{1}H spectrum over the sensitive volume of the ^{13}C coil, when placing the carrier frequency in the middle of the ^{1}H spectrum at 3 ppm.

Proton decoupling was applied for the entire acquisition time of 171 μs. In combination with the repetition time (TR) of 3 s, an average total power deposition of 1.7 Watts due to decoupling was achieved. When taking into account all the pulses used in the sequence (Fig. 1) and their respective contribution to the average power, a maximum average power deposition of 3 Watts was calculated, neglecting radiation losses and losses in the coil. When taking into account that the RF coil covers approximately a 2-liter volume, the total SAR dissipated into the sensitive volume of the ^{1}H coil is thus calculated to be less than 2 W/kg, which is well within absorption guidelines. Local specific RF absorption rates were estimated for a 10-cm diameter loop in the occipital lobe assuming the maximum γB_1 at the coil center (500 Hz) and a tissue conductivity of 0.8 Siemens/m at 170 MHz (21) based on Faraday's Law. This calculation is equivalent to using the vector potential model (9). According to these calculations, local RF power deposition for the whole sequence was at most 3 W/kg. This value is well below the recommended maximum local SAR of 4 W/kg for the head. We have restricted our initial experiments to the occipital lobe, which is a cortical brain region with high blood flow, and thus maximal local heat exchange with the entire blood pool and body.

The pulse sequence used for localizing the ^{13}C signals is shown in Fig. 1, for which we propose the acronym PRECISELY (PRoton Excited C-13 Image SElected *in vivo* Localized spectroscopY). Localization was based on the image-selected *in vivo* spectroscopy (ISIS) scheme (22) indicated by the dotted pulses in the dashed box. For inversion of the ^{1}H z magnetization, phase-swept hyperbolic secant (sech) pulses (see ref. 3 and references therein) of 6.6 μs duration were used, which gave a nominal band width of 3 kHz. The thus prepared ^{1}H z magnetization was transferred to ^{13}C by using polarization transfer according to the distortionless enhanced polarization transfer (DEPT) scheme (23). The delays, which were nominally equal to $1/2J_{CH}$ were set for either J_{CH} = 135 Hz for the observation of CH_2 groups or J_{CH} = 155 Hz for observation of CH resonances based on J_{CH} measurements in phantoms. The flip angle of the third pulse, θ, can be used to edit the spectrum for detecting just the CH resonances (θ = 90°), or for detecting the CH_2 and CH_3 resonances at maximum sensitivity and the CH resonances with 70% sensitivity (θ = 45°). Simulations of the DEPT sequence based on the measured RF profile of the ^{1}H coil indicated that equal sensitivity can be

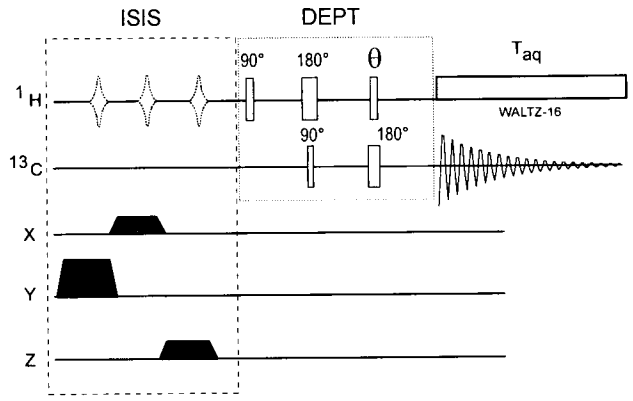

FIG. 1. Pulse sequence used to localize ^{13}C NMR signals. Volume selection was achieved by ISIS (22) applied to the proton *z* magnetization as indicated in the dashed box. The ^1H *z* magnetization was then transferred to ^{13}C using DEPT (23) by using hard pulses (dotted box). The nominal flip angle of the third proton pulse (θ) was set to 90° to edit for signals from CH groups only, or to θ = 45° to detect all CH_n groups. During the acquisition time of 171 μs, WALTZ-16 decoupling was applied at 30 W with a 670-μs 90° pulse element. The repetition time *TR* was 3 s. We propose the acronym PRECISELY (PRoton Excited C-13 Image SElected *in vivo* Localized spectroscopY) for these localization schemes.

achieved for CH_2 carbons when using θ = 45° as for the CH carbons using θ = 90°.

Since the DEPT sequence contains spin-echo pulse sequence elements on both frequencies, it is highly sensitive to B_1 and B_2 variations and thus requires careful calibration of pulse widths, especially when using hard pulses in combination with surface coils. An early report proposing use of proton localization methods combined with DEPT used homogenous RF coils (24). Pulse widths and power settings in the present study were based on the relative position and the RF calibration performed on the signal of the formate sphere as described above. Decoupler and transmitter (^{13}C) pulse widths depended on the depth of the localization with respect to the coil center and were calibrated by using aqueous natural abundance glucose (250 m*M*), *myo*-inositol (100 m*M*), glutamate (50 m*M*), glutamine (50 m*M*), and taurine (50 m*M*) phantoms. The solutes were placed into an aqueous solution of 100 m*M* NaCl.

The calibration of decoupler pulse widths confirmed that the ^1H RF field was maximal at the ^{13}C coil center. These calibrations gave a 300-μs 90° pulse width 5 cm into the sample when the 90° pulse width at the ^{13}C coil center was 250 μs, which is a 20% drop in B_2, thereby further illustrating the excellent B_2 homogeneity of the coil assembly. Unlocalized spectra were acquired with NOE generation using either a hard pulse for excitation or a numerically optimized adiabatic sin/cos pulse (25).

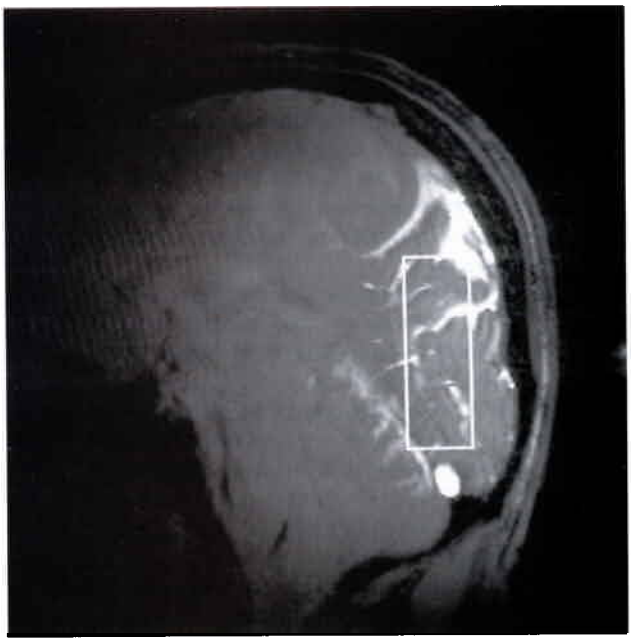

a

b

FIG. 2. Volume localization in the occipital cortex. The figure shows FLASH MRI of the human head (18). The box indicates the position of the volume localized for the present study. The field of view was 20 cm, the repetition time (*TR*) was 60 μs, the echo time (*TE*) 7 μs, 5-mm slice thickness. A 90° flip angle was used at the carbon coil center. (a) shows a sagittal image, (b) shows an axial image. The volume indicated has the dimensions 6 × 2 × 6 cm (72 ml).

RESULTS

Figure 2 shows sagittal and axial FLASH images of the human head acquired with a 90° flip angle at the coil center (*TR* = 60 μs, *TE* = 7 μs). Most of the signal intensity in the image is therefore between linearly and quadratically proportional to B_1, and the fact that signal up to the frontal region was observed (not shown in this gray scale) demonstrates the excellent RF homogeneity available for ^1H decoupling with this semi-volume coil.

To demonstrate that the localization method presented in Fig. 1 is efficient in localizing the entire ^{13}C spectrum of proton coupled nuclei, we acquired an unlocalized

spectrum and compared it with one acquired with θ = 45°. This choice of θ ensured detection of all proton-coupled ^{13}C nuclei with comparable sensitivity. The comparison is shown in Fig. 3. The localized spectrum (bottom) shows that the localization eliminated all lipid signals over the entire chemical shift range of coupled ^{13}C resonances, i.e., 150 ppm. A closer inspection of the localized spectrum revealed that the strong CH_2 signal at 30.5 ppm was eliminated to the level of natural abundance metabolites.

To further compare unlocalized spectra with localized spectra, Fig. 4a shows a spectral expansion covering the 35–85 ppm range. The localized spectrum (top) was acquired from one subject in 36 min by using the sequence in Fig. 1 with θ = 90°. The peaks from Glu, NAA, and the *myo*-inositol single carbon intensities were observed with a signal-to-noise ratio of approximately 8:1. The concentration of Glu, NAA, and *myo*-inositol is on the order of 7–9 μmol/g in the human brain, see ref. 5 and references therein. Therefore, this sensitivity translates into a signal-to-noise ratio of approximately 2:1 $mM^{-1}h^{-1/2}$ for these 72-ml volumes. The bottom spectrum was acquired by using a pulse-and-acquire sequence with 1 W NOE generation during the recovery period. Resolved signals, most prominently those from the glycerol moiety of triacylglycerol fat at 62 and at 69 ppm were observed with a 20–30 Hz linewidth, which is comparable with all lipid resonances. In addition, four sharp resonances due to *myo*-inositol were observed between 72 and 76 ppm, several peaks at 55 ppm and two peaks at 40.5 ppm.

Figure 4b shows an additional expansion of the spectral region at 68–78 ppm and at 50–60 ppm. The resolved peaks from *myo*-inositol at 72, 73, 73.3, and 75 ppm, as well as resolved peaks from the C2 of glutamate (Glu) at 55.6 ppm and the C2 of *N*-acetyl-aspartate (NAA) at 54.0 ppm (26, 27) can be clearly identified. The unlocalized spectra (bottom) show a peak from glutamine (Gln) at 55.1 ppm that is resolved from the choline methyl peak (Cho) at 54.9 ppm, which overlaps with the methylene carbon of creatine (Cr) at 54.7 ppm. The localized spectrum (top) clearly shows several effects of the localized polarization transfer sequence. First, the intense glycerol signals from scalp lipids were eliminated due to the localization process and, second, the signals from the Cr methylene and Cho methyl at 54.7 ppm were eliminated as well, due to θ being 90°.

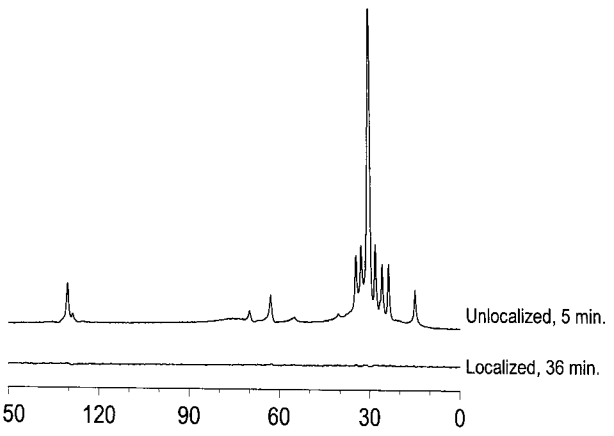

FIG. 3. Comparison of a localized with an unlocalized ^{13}C spectrum. The top trace shows the entire bandwidth of CH_n signals of an unlocalized ^{13}C NMR spectrum from the human head. This spectrum was acquired in 7 min with an adiabatic sin/cos pulse by using a numerically optimized modulation function (25) as in previous ^{13}C MRS studies (3). The bottom spectrum was acquired for 36 min by using the pulse sequence of Fig. 1 (θ = 45°) from a 72-ml volume exactly as in Fig. 2. Power absorption was calculated to be below 3 W. Both spectra are shown without baseline correction and were processed with 5 Hz exponential multiplication.

These spectra demonstrate the high spectral resolution achieved at 4 Tesla. The metabolite linewidths were in some spectra as low as 2 to 3 Hz, as assessed by measuring peak widths in linebroadened spectra and by fitting Lorentzian peaks to the spectrum and by taking the applied 3 Hz line broadening into account.

The high sensitivity of ^{13}C MRS at 4 Tesla was further evident from the observation of peak intensity of Gln at 55.1 ppm above the noise floor in 12-min acquisition time and the observation of *myo*-inositol after 3 min acquisition (not shown). Assuming a 4-m*M* cerebral Gln concentration in normal human brain (5), this sensitivity indicates that the detection limit is on the order of 0.02–0.04 m*M* in ^{13}C concentration.

DISCUSSION

A major obstacle to apply ^{13}C MRS to humans is the requirement to use ^{1}H decoupling, which simplifies the spectra considerably and increases the signal-to-noise ratio substantially. However, the concomitant requirement that the RF power deposition be within the absorption guidelines imposes a restriction that has been considered to limit broadband decoupling to 1.5 Tesla even when using special precautions (9, 13, 14). Such a restriction is usually not present in animal and *in vitro* experiments, which may explain the wealth of animal studies (e.g., ref. 16 and references therein) contrasting the few human brain studies reported in the literature, see above. It is generally assumed that with increasing static field strength, RF power deposition increases with B_o^2 (9). In addition to this B_o^2 dependence, an additional B_o^2 dependence is added, since the bandwidth that needs to be decoupled increases linearly with B_o. The present peak power requirements are 30 Watts for a 700–900 Hz band width at 4 Tesla, which is comparable with the 13 W used at 2.1 Tesla in the human brain for covering a 400-Hz bandwidth (5) and to the 35 W used at 1.5 T for covering an 850-Hz band width (13). We therefore conclude that the power per unit bandwidth appears to increase less than quadratically with the field. A possible explanation is that the present quadrature coil design (20), which has not yet been attempted at 1.5–2.1 Tesla, may represent a significant improvement over previous designs. The fact that similar RF power was needed to cover equivalent bandwidths as previously at 1.5 Tesla using less homogenous coils (13, 14) indicates that local hot spots are substantially reduced compared with linearly polarized surface coils. Furthermore, the total specific absorption rate measured at the coil port, i.e., 3

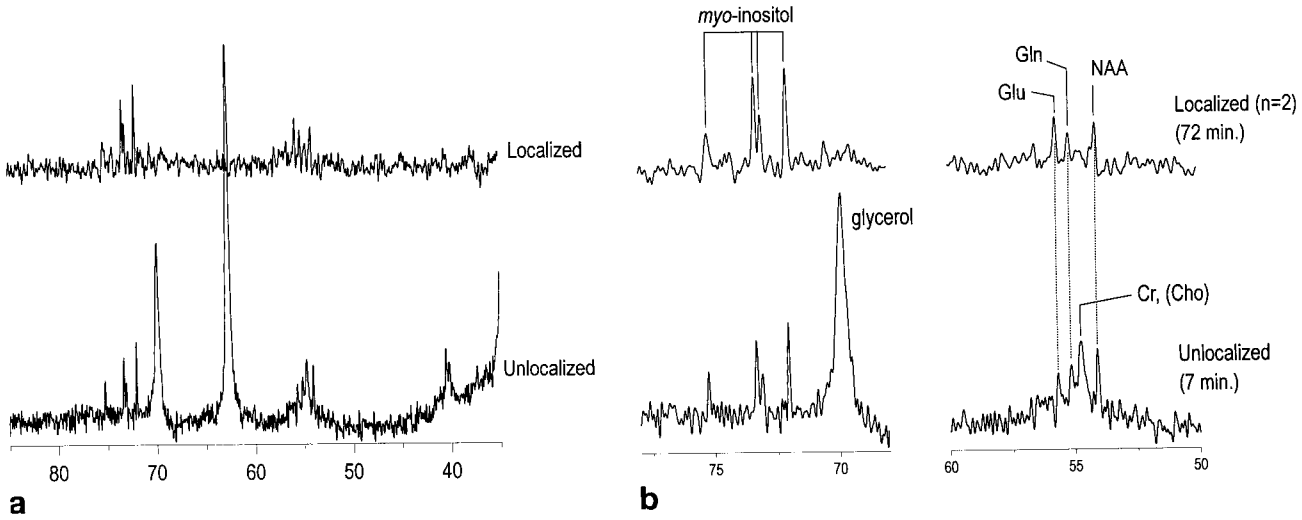

FIG. 4. Effect of ^1H NMR localization on the ^{13}C spectrum. Shown is the 35- to 85-ppm chemical shift range (a) comparing an unlocalized spectrum acquired with NOE generation (bottom) to that acquired with the sequence of Fig. 1 using $\theta = 90°$. The unlocalized spectrum shows signal intensity from two peaks at 40.5 ppm, consistent with the chemical shift of NAA plus GABA. A comparison is shown in (b). Peaks from *myo*-inositol at 72.02, 73.0, 73.3, and 75.1 ppm, as well as the glutamate C2 at 55.7 ppm, Gln C2 at 55.1 ppm, and NAA at 54.0 ppm are clearly observed. The peaks from creatine (54.6 ppm) and choline (54.8 ppm) overlap at 54.7 ppm and are eliminated by the polarization transfer that was set to detect CH groups ($\theta = 90°$). The localized spectrum (top) is the pooled spectrum from two subjects (one 72-ml and one 108-ml volume with a total acquisition time of 72 min or 1536 transients). Processing consisted of a mild Lorentzian to Gaussian conversion (2 Hz) and zero-filling. No baseline correction was applied. Peak assignments are according to refs. 26, 27.

Watts, provides a physical upper limit for the SAR integrated over the sensitive volume of the coil (1.5–2 liters). We estimated the local SAR to be below 3 W/kg (see Methods), assuming a uniform spatial distribution of the maximal RF amplitude in the sample. In other words, an improved spatial uniformity at equal total RF power dissipation implies that maximal local SAR is substantially reduced. Our calculations show that even under worst case assumptions the FDA guidelines are easily met at 4 Tesla.

We have used a rather straightforward polarization transfer scheme, namely DEPT (23) in combination with three-dimensional ISIS (22) localization of the proton z magnetization as shown in Fig. 1. This sequence has permitted properly localizing the entire ^{13}C spectrum to the brain as is evident from the elimination of resonances from scalp triacylglycerol over the entire chemical shift range shown in Fig. 3. This simultaneous observation of the entire ^{13}C NMR spectrum extends our previous observations that mobile triacylglycerol ^{13}C NMR resonances represent a contamination from scalp fat and bone, which can be eliminated by using 3D localization (2, 3, 5). Studies of *in vivo* brain metabolism using ^{13}C NMR detection that relied on more crude localization means may thus not be representative of brain tissue *per se*, as judged from the dominant presence of lipid signals.

At 2.1 Tesla using direct ISIS ^{13}C localization in combination with B_1 insensitive pulses and NOE generation (3), the estimated sensitivity was 0.8 $mM^{-1}h^{-1/2}$ at natural abundance, which was consistent with the experience that signals from *myo*-inositol (which constitute approximately 14 m*M* concentration for the degenerate resonances) could be observed after 60 min of data accumulation from these large volumes (3) and that natural abundance NAA was observable at 40.5 ppm (unpublished data). Currently, we can detect approximately 4 m*M* Gln after 12 min of data accumulation at 4 Tesla in a 72-ml volume (not shown). For a 144-ml volume, the signal-to-noise ratio is predicted at 4 Tesla to be approximately 4.5:1 $mM^{-1}\ h^{-1/2}$ at natural abundance, which constitutes a five- to sixfold improvement in sensitivity compared with 2.1 Tesla. This sensitivity estimate suggests that natural abundance ^{13}C MRS at 4 Tesla might be useful in estimating concentrations of metabolites in the m*M* concentration range. Metabolites such as taurine, aspartate, *scyllo*-inositol, GABA, glutathione, and *N*-acetyl-aspartyl-glutamate (NAAG), which might have concentrations in the millimolar range, could potentially be estimated by using pooled natural abundance measurements. Such an estimate by natural abundance ^{13}C NMR can help in the interpretation and quantification of the extremely crowded ^1H NMR spectrum, as we have previously suggested with *myo*-inositol (3). In addition, metabolites present in the submillimolar concentration could potentially be quantified by using ^{13}C enrichment of a few percent suggesting that ^{13}C tracer experiments are now feasible.

From the above signal-to-noise ratio measurements, we expect that for a 12-ml volume the rms noise amplitude in 4-min acquisitions is equivalent to a natural abundance signal of 15 m*M*. In other words, the noise level for 4 min of data accumulation should correspond to 0.16 m*M* [^{13}C]. It should therefore be possible to perform localized ^{13}C NMR of activated cortical areas with a reasonable time resolution, since Glu, Gln, and glucose have been shown to be labeled with concentrations between 1.7–2.5 m*M* by using [1-^{13}C] D-glucose infusions (5). Further potential improvements in sensitivity might be possible by incorporating B_1 insensitive pulses (28, 29). In addition, infusion of [1,6-$^{13}C_2$]-labeled glucose

should permit increasing the time resolution and/or decreasing the volume size even further and would also permit studying isotopomer patterns in low concentration metabolites, such as GABA and aspartate, in the human brain.

CONCLUSIONS

The present paper demonstrates that broadband decoupling is feasible at 4 Tesla within absorption guidelines and demonstrates the *in vivo* localization efficiency of ^{1}H localization combined with polarization transfer in the human brain. The observed linewidths suggest that ^{13}C linewidths do not increase substantially with static field strength and that the sensitivity at 4 Tesla should permit studying the effects of focal activation on brain metabolism in conjunction with ^{13}C label infusion.

ACKNOWLEDGMENTS

The authors thank Kamil Ugurbil for his support and encouragement.

REFERENCES

1. F. A. Howe, R. J. Maxwell, D. E. Saunders, M. M. Brown, J. R. Griffiths, Proton spectroscopy in vivo. *Magn. Reson. Q.* **9,** 31–59 (1993).
2. R. Gruetter, E. J. Novotny, S. D. Boulware, D. L. Rothman, G. F. Mason, G. I. Shulman, R. G. Shulman, W. V. Tamborlane, Direct measurement of brain glucose concentrations in humans by ^{13}C NMR spectroscopy. *Proc. Natl. Acad. Sci. USA* **89,** 1109–1112 (1992).
3. R. Gruetter, D. L. Rothman, E. J. Novotny, R. G. Shulman, Localized ^{13}C NMR spectroscopy of *myo*-inositol in the human brain in vivo. *Magn. Reson. Med.* **25,** 204–210 (1992).
4. G. F. Mason, R. Gruetter, D. L. Rothman, K. L. Behar, R. G. Shulman, E. J. Novotny, Simultaneous determination of the rates of the TCA cycle, glucose utilization, α-ketoglutarate/glutamate exchange, and glutamine synthesis in human brain by NMR. *J. Cereb. Blood Flow Metab.* **15,** 12–25 (1995).
5. R. Gruetter, E. J. Novotny, S. D. Boulware, G. F. Mason, D. L. Rothman, J. W. Prichard, R. G. Shulman, Localized 13C NMR spectroscopy of amino acid labeling from [1–13C] D-glucose in the human brain. *J. Neurochem.* **63,** 1377–1385 (1994).
6. R. Fried, N. Beckmann, U. Keller, R. Ninnis, G. Stalder, J. Seelig, Early glycogenolysis and late glycogenesis in human liver after intravenous administration of galactose. *Am. J. Physiol.* **33,** G14–G19 (1996).
7. R. Gruetter, I. Magnusson, D. L. Rothman, M. J. Avison, R. G. Shulman, G. I. Shulman, Validation of ^{13}C NMR determination of liver glycogen *in vivo*. *Magn. Reson. Med.* **31,** 583–588 (1994).
8. D. L. Rothman, I. Magnusson, L. D. Katz, R. G. Shulman, G. I. Shulman, Quantitation of hepatic glycogenolysis and gluconeogenesis in fasting humans with ^{13}C NMR. *Science* **254,** 573–576 (1991).
9. P. A. Bottomley, C. J. Hardy, P. B. Roemer, O. M. Mueller, Proton-decoupled, Overhauser-enhanced, spatially localized carbon-13 spectroscopy in humans. *Magn. Reson. Med.* **12,** 348–363 (1989).
10. H. Bomsdorf, P. Roschmann, J. Wieland, Sensitivity enhancement in whole-body natural abundance ^{13}C spectroscopy using ^{13}C/^{1}H double-resonance techniques at 4 Tesla. *Magn. Reson. Med.* **22,** 10–22 (1991).
11. N. Beckmann, I. Turkalj, J. Seelig, U. Keller, ^{13}C NMR for the assessment of human brain glucose metabolism in vivo. *Biochemistry* **30,** 6362–6366 (1991).
12. P. Bachert, M. E. Bellemann, M. Layer, T. Koch, W. Semmler, W. J. Lorenz, ^{31}P-[^{1}H] and ^{13}C-[^{1}H] magnetic resonance spectroscopy of malignant histiocytoma and skeletal muscle tissue in man. *NMR Biomed.* **5,** 161–170 (1992).
13. A. Heerschap, P. R. Luyten, J. I. van der Heyden, L. J. M. P. Oosterwaal, J. A. den Hollander, Broadband proton decoupled natural abundance ^{13}C NMR spectroscopy of humans at 1.5 Tesla. *NMR Biomed.* **2,** 1–10 (1989).
14. N. Beckmann, J. Seelig, H. Wick, Analysis of glycogen storage disease by *in vivo* ^{13}C NMR: comparison of normal volunteers with a patient. *Magn. Reson. Med.* **16,** 150 (1990).
15. M. Saner, G. McKinnon, P. Boesiger, Glycogen detection *in vivo* ^{13}C NMR: a comparison of proton decoupling and polarization transfer. *Magn. Reson. Med.* **28,** 65–73 (1991).
16. H. Bachelard, R. Badar-Goffer, NMR spectroscopy in neurochemistry. *J. Neurochem.* **61,** 412–429 (1993).
17. J. H. Lee, M. Garwood, R. Menon, G. Adriany, P. Andersen, C. L. Truwit, K. Ugurbil, High contrast and fast three-dimensional imaging at high fields. *Magn. Reson. Med.* **34,** 308–312 (1995).
18. A. Haase, J. Frahm, D. Matthaei, W. Hänicke, K. D. Merboldt, FLASH Imaging. Rapid NMR imaging using low flip-angle pulses. *J. Magn. Reson.* **67,** 258–266 (1986).
19. R. Gruetter, Automatic, localized in vivo adjustment of all first- and second-order shim coils. *Magn. Reson. Med.* **29,** 804–811 (1993).
20. G. Adriany, K. Ugurbil, R. Gruetter, A surface coil design for efficient proton decoupling in humans, *in* "Proc., ISMRM, 4th Annual Meeting, New York, 1996," p. 1431.
21. H. Barfuss, H. Fischer, D. Hentschel, R. Ladebeck, A. Oppelt, R. Wittig, W. Duerr, R. Oppelt, In vivo magnetic resonance imaging and spectroscopy of humans with a 4T whole body magnet. *NMR Biomed.* **3,** 31–45 (1990).
22. R. J. Ordidge, A. Connelly, J. A. B. Lohman, Image-selected in vivo spectroscopy (ISIS). A new technique for spatially selective NMR spectroscopy. *J. Magn. Reson.* **66,** 283–294 (1986).
23. D. M. Doddrell, D. T. Pegg, M. R. Bendall, Distortionless enhancment of NMR signals by polarization transfer. *J. Magn. Reson.* **48,** 323–327 (1982).
24. W. P. Aue, S. Mueller, J. Seelig, Localized ^{13}C NMR spectra with enhanced sensitivity obtained by volume-selective excitation. *J. Magn. Reson.* **61,** 392–395 (1985).
25. K. Ugurbil, M. Garwood, A. Rath, Optimization of modulation functions to improve insensitivity of adiabatic pulses to variations in B_1 magnitude. *J. Magn. Reson.* **80,** 448–469 (1988).
26. M. Bárány, C. Arús, Y. C. Chang, Natural abundance ^{13}C NMR of brain. *Magn. Reson. Med.* **2,** 289–295 (1985).
27. W. Willker, J. Engelmann, A. Brand, D. Leibfritz, Metabolite identification in cell extracts and culture media by proton-detected 2D-H,C-NMR spectroscopy. *J. MR Anal.* **2,** 21–32 (1996).
28. H. Merkle, H. Wei, M. Garwood, K. Ugurbil, B_1 insensitive heteronuclear adiabatic polarization transfer for signal enhancement. *J. Magn. Reson.* **99,** 480–494 (1992).
29. S.-G. Kim, M. Garwood, Double DEPT using adiabatic pulses. Indirect heteronuclear T1 measurement with B1 insensitivity. *J. Magn. Reson.* **99,** 660–667 (1992).